



Brief Communication: Conventional assumptions involving the speed of radar waves in snow introduce systematic underestimates to sea ice thickness and seasonal growth rate estimates

Robbie D.C. Mallett¹, Isobel R. Lawrence¹, Juliennne C. Stroeve^{1,2,3}, Jack C. Landy⁴, and Michel Tsamados¹

¹Centre for Polar Observation and Modelling, Earth Sciences, University College London, London, UK

²National Snow and Ice Data Center, University of Colorado, Boulder, CO, USA

³Centre for Earth Observation Science, University of Manitoba, Winnipeg, Canada

⁴School of Geographical Sciences, University of Bristol, Bristol, UK

Correspondence: Robbie Mallett (robbie.mallett.17@ucl.ac.uk)

Abstract.

Pan-Arctic sea ice thickness has been monitored over recent decades by satellite radar altimeters such as CryoSat-2, which emit Ku-band radar waves that are conventionally assumed to penetrate overlying snow and scatter from the ice-snow interface. Here we examine two expressions for the time delay caused by slower radar wave propagation through the snow layer and related assumptions concerning the time-evolution of overlying snow density. Two conventional treatments lead to systematic underestimates of winter ice thickness and thermodynamic growth rate of up to 15 cm over multiyear ice. Correcting these biases would improve the accuracy of sea ice thickness products, which feed a wide variety of model projections, calibrations, validations and reanalyses.

1 Introduction

Sea ice is a key moderator of the global climate system, limiting the exchange of heat, moisture and momentum fluxes between the ocean and the atmosphere. It also plays a crucial role in ocean circulation and Arctic Ocean primary productivity (e.g. Sévellec et al., 2017; Chan et al., 2017). During autumn, open water areas form new ice that can grow thermodynamically by 1.5 to 2.5 m over a winter season. Ridging and rafting can locally increase the ice thickness and, if the ice survives the following melt season, further deformation and thermodynamic ice growth can lead to thicknesses in excess of 5 m.

Today the Arctic is undergoing a period of profound transformation, with the area and thickness of the floating sea ice cover in rapid decline (e.g. Stroeve and Notz, 2018; Kwok, 2018). These changes are partially a result of a distinct change in seasonality in the Arctic with the melt season starting earlier and lasting longer, enhancing the ice-albedo feedback (Stroeve and Notz, 2018). Delays in freeze-up have reduced both the amount of snow that accumulates on the sea ice over winter (Stroeve et al., 2019; In Revision), and together with recent increases in winter air temperatures, have reduced the rate of thermodynamic ice growth (Graham et al., 2017; Stroeve et al., 2018). Winter sea ice thickness also functions as a prognostic variable in the polar climate system, affecting the amount and distribution of sea ice that will survive the summer melt season. Accurate



knowledge of sea ice thickness is particularly important where data are assimilated into forecasting systems and other complex models which often exhibit sensitive dependence on initial conditions (Day et al., 2014).

Sea ice thickness has been observed through various methods including submarines, ice mass-balance buoys, electromagnetic induction sounding and satellite laser and radar altimetry (e.g. Schweiger, 2017; Kwok, 2018). The CryoSat-2 mission has played a leading role over the last decade, providing radar ranging observations from which the sea ice thickness may be derived (Wingham et al., 2006; Laxon et al., 2013; Tilling et al., 2018).

Ku-band radar altimeters such as CryoSat-2 and Sentinel-3 do not directly measure sea ice freeboard, but instead measure ‘radar freeboard’ through a time-of-flight calculation. The radar freeboard is the difference in radar ranging between the snow-ice interface and the local, instantaneous sea level (assuming perfect radar wave penetration through the snowpack). Since the radar wave speed is reduced in snow, a priori knowledge of the snow depth and density is required to convert the radar freeboard to the true ice freeboard. Following the freeboard calculation, sea ice thickness can then be estimated through the assumption of hydrostatic equilibrium (e.g. Laxon et al., 2003). This again requires a priori knowledge of snow depth and density to account for freeboard reduction due to the weight of overlying snow. The magnitude of freeboard correction for the weight of overlying snow is typically twelve times that for the effect of slower wave propagation in snow.

An important consideration in the conversion of radar freeboard (F_r) to ice freeboard (F_i) and in turn ice thickness is therefore the time delay due to slower radar pulse propagation in snow (Kwok, 2014). In this study we highlight two different approaches to the calculation of this time delay used in published literature. Correct handling of this time delay has a significant impact on the retrieval of sea ice thickness and volume from radar altimetry, as we show here. This is particularly the case as snow settles and densifies over the winter season.

We further investigate the impact of assuming a fixed snow density throughout winter when calculating this time delay. At present no groups producing publicly available sea ice thickness products from CryoSat-2 factor monthly evolution of snow density into their correction for slower radar wave propagation in snow, despite often including an evolving density in their calculation of the floe’s hydrostatic equilibrium. The impact of this assumption is assessed and found to produce underestimates of the rate of winter thermodynamic sea ice growth, with October-April growth currently being underestimated by over 10 cm over multiyear ice.

2 Different Treatments of the Radar Propagation Correction

The correction to the radar range to account for slower radar wave propagation in snow, $\delta h = F_i - F_r$, is often expressed as the product of snow depth, Z , and some function of wave velocity in snow, $f(c_s)$ (e.g. Tilling et al., 2018; Kwok, 2014) such that:

$$\delta h = Z \times f(c_s) \quad (1)$$

We now present a short derivation of $f(c_s)$ and thus δh through consideration of the extra time taken, δt , for a radar wave to travel a distance Z through a specified snow depth rather than through free space. The time delay induced by the snow layer is expressed:



$$\delta t = t_{snow} - t_{vacuum} \quad (2)$$

$$55 \quad \delta t = Z/c_s - Z/c \quad (3)$$

$$\delta t = Z(1/c_s - 1/c) \quad (4)$$

Where c_s the wave speed in snow, and c is the radar wave speed in free space ($3 \times 10^8 \text{ ms}^{-1}$). To convert this time delay (δt) into a path difference (δh), one multiplies by the speed of the wave in free space:

$$\delta h = \delta t \times c = Z(c/c_s - 1) \quad (5)$$

60 Tilling et al. (2018) use this formulation to correct the radar range for the slower propagation speed through snow. Some authors have used an alternative form of Eq. 5, generated by multiplying δt in Eq. 4 by the wave speed in snow (Kwok, 2014; Kurtz et al., 2014; Kwok and Cunningham, 2015; Ricker et al., 2015; Armitage and Ridout, 2015; Hendricks et al., 2016; Landy et al., 2017; Xia and Xie, 2018):

$$\delta h = Z_r(1 - c_s/c) \quad (6)$$

65 For Eq. 6 to be true, Z_r must be regarded as:

$$Z_r = Z(c/c_s) \quad (7)$$

However, Z_r is conventionally interpreted as the real snow depth (Z) and δh is therefore erroneously reduced by a factor of c_s/c . When Eq. (7) is incorporated into Eq. (6), δh is redefined in terms of Z and becomes Eq. (5).

Conventional interpretation of Z_r as the real snow depth therefore leads to a bias in the freeboard (B_f) where:

$$70 \quad B_f = Z \times \frac{(c - c_s)^2}{c \times c_s} \quad (8)$$

Bias in the freeboard then propagates into estimates of sea ice thickness by a multiplicative factor of $\rho_w/(\rho_w - \rho_i)$, where ρ_w represents the density of seawater and ρ_i represents the density of sea ice. Because first year ice (FYI) is generally denser than multiyear ice (MYI), a fixed snow thickness will cause a greater bias on the thickness of first year ice. However, typical biases over FYI are generally expected to be lower due to reduced snow accumulation. The bias in sea ice thickness (B_{SIT})

75 due to conventional, erroneous use of Eq. (6) is therefore:

$$B_{SIT} = Z \times \frac{(c - c_s)^2}{c \times c_s} \times \frac{\rho_w}{\rho_w - \rho_i} \quad (9)$$



Equation 9 illustrates that the bias grows linearly with snow depth. In addition to this, B_{SIT} is also dependent on the speed of the radar wave in snow, which is itself a function of snow density. Several empirical relationships have been proposed for the relationship between snow density and radar wave speed, however the most commonly used three (Hallikainen et al., 1982; Tiuri et al., 1984; Ulaby et al., 1986) deviate negligibly from each other in the typical density range for snow observed on Arctic sea ice (Fig. S1). In this investigation, we use the relationship from Ulaby et al. (1986):

$$c_s = c(1 + 0.51\rho_s)^{-1.5} \quad (10)$$

As snow density increases, c_s decreases and B_{SIT} increases. This positive relationship between $f(c_s)$ and snow density is shown in Fig. 1a. Because both snow depth and snow density generally increase throughout the season as snow accumulates, compacts and settles, any δh generated through incorrect expression of $f(c_s)$ becomes increasingly underestimated.

Furthermore, B_{SIT} increases even as a fixed snow water equivalent densifies and shrinks in volume. This is because B_{SIT} scales more rapidly with increasing snow density than it reduces with decreasing snow depth. The increase in bias with snow density for constant SWE is illustrated in Fig. 1b.

Since B_{SIT} is explicitly a function of snow depth and implicitly a function of snow density via Eq. (10), its spatial mapping requires the use of an Arctic snow distribution. Here we use snow depths and densities from Warren et al. (1999) (henceforth ‘W99’) to illustrate these underestimates. To be consistent with current data products that rely on W99 for their snow depth distribution, we halve snow depths over first-year ice as per Laxon et al. (2013) and only consider the Central Arctic basin (see Fig. S2) where W99 is considered most reliable (Kwok and Cunningham, 2015). Data on sea ice type and extent were taken from the sea ice type product of the EUMETSAT Ocean and Sea Ice Satellite Application Facility (OSISAF; Aaboe et al., 2016).

We find that where sea ice thicknesses are calculated using W99 snow depths and densities in the Central Arctic, thickness underestimates increase throughout the winter to values exceeding 15 cm in April over multi-year ice (Fig. 1c). Over FYI the mean bias increases from 4.2 cm in October to 9.8 cm in April (compared to 6.4 cm and 13.6 cm for MYI). In April, 28% of MYI has a bias exceeding 15 cm, and 7% exceeds 16 cm.

How does this bias impact sea ice thickness products currently available to the science community? Most commonly-used products do not correct for slower wave speed using the W99 density distributions in time or space, but instead use a reference density to calculate a fixed value for $f(c_s)$ in Eq. (1). This value is fixed not only across the Arctic basin, but throughout the winter. In the CryoSat-2 sea ice thickness product from the Alfred Wegener Institute (AWI; Hendricks et al., 2016), $f(c_s)$ is taken as $(1 - c_s/c)$ as in Eq. (6). Citing the reference spring snow density given by Kwok (2014) of 350 kg m^{-3} , they generate a fixed δh of $0.22Z$.

On the other hand, the Centre for Polar Observation and Modelling (CPOM) takes $f(c_s)$ to be $(c/c_s - 1)$ (Eq. (5); Tilling et al., 2018). However, the CPOM product uses a lower reference density of 300 kg m^{-3} (taken from (Kwok et al., 2011)), generating a reference δh of $0.25Z$. AWI’s use of a higher reference density mitigates the difference introduced by their

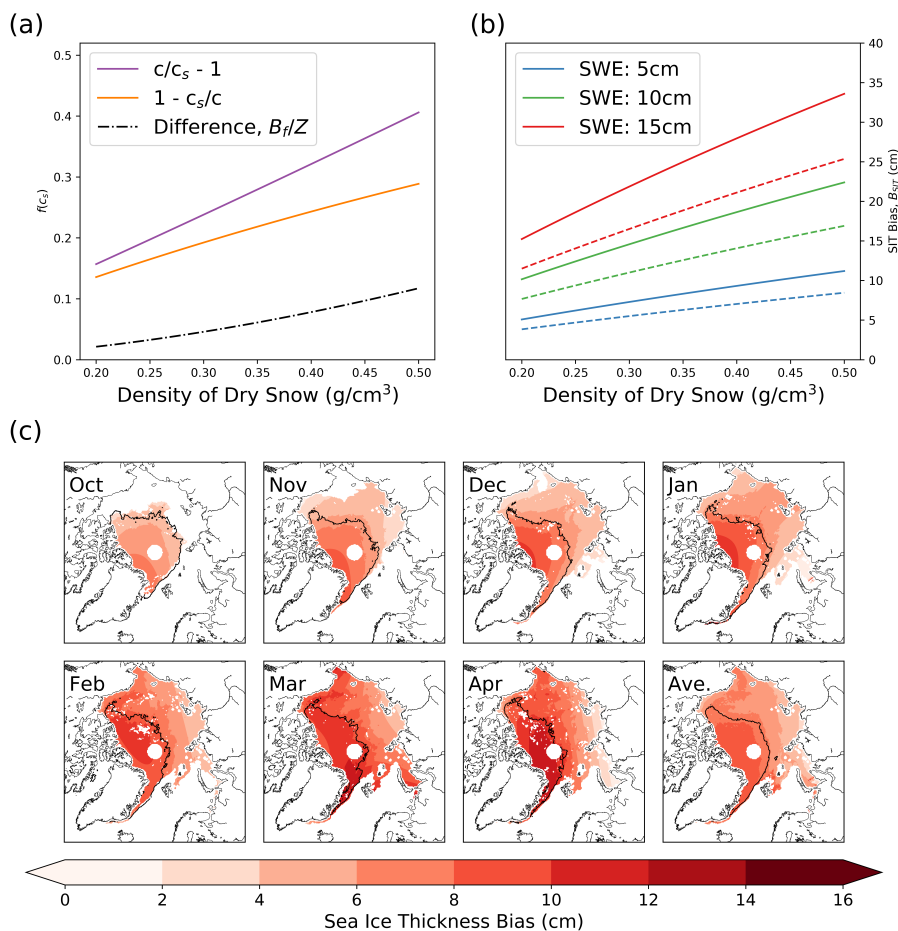


Figure 1. (a) Difference between conventional use of Eq. (6) and Eq. (5) as a function of snow density. This bias increases with snow density, ultimately exceeding a factor of 0.1 of the snow depth for dense snow. (b) Sea ice thickness bias for a fixed mass of snow increases as it densifies and contracts with time. Solid lines indicate bias for first year ice, dashed lines for multiyear ice assuming fixed densities of 916.7 and 882 kg m^{-3} respectively. (c) Monthly thickness bias introduced by conventional and erroneous use of Eq. (6) when calculated using W99 density and depth distributions. Pixels are only displayed where sea ice type is known in all years 2010-2018. Black line indicates region where multiyear ice is present in over 50% of years. Monthly averages derived from years 2010-2018.

erroneous interpretation of Eq. (6). Were AWI to use a similar reference density to CPOM's 300 kg m^{-3} with Eq. (6), their reference δh would be $0.19Z$, contrasting starkly with CPOM's $0.25Z$.

The decision to use a fixed snow density for the wave-speed propagation correction throughout the winter introduces biases of its own with regard to the rate of thermodynamic growth; this is discussed in the next section.



3 Impact of Seasonal Snow Density Evolution on the Radar Wave Propagation Correction

Despite recent and significant developments in pan-Arctic scale snow density modelling (e.g. Stroeve et al., In Revision; Petty et al., 2018b), the Arctic snow density distribution remains poorly constrained in time and space. Because of this, representative values for pan-Arctic average snow density are often combined with the snow depth distributions from W99 to calculate the radar wave propagation correction (Kurtz et al., 2014; Hendricks et al., 2016; Tilling et al., 2018).

To investigate the impact of an evolving snow density on freeboard conversions, we calculated the wave-speed correction over Arctic sea ice by two methods: The control method used a fixed reference density in the wave speed correction (i.e. 300 kg m⁻³) as done by CPOM and AWI. The other method incorporated a rate of snow densification obtained from the Central Arctic data published in W99.

The control method used the parameters employed by Tilling et al. (2018) producing a radar wave speed in snow of 2.4x10⁸ m s⁻¹ corresponding to a reference density of 300 kg m⁻³ when converted using Eq. (10). As discussed in Sect. 2, estimates of absolute sea ice thickness are sensitive to the choice of reference snow density. However, the estimated rate of thermodynamic growth (the focus of this section) is more responsive to the density's time derivative, which for a fixed value ($\rho_s = 300 \text{ kg m}^{-3}$) is zero. As such, our results are applicable to different reference densities such as those used by AWI (350 kg m⁻³) and the NASA Goddard Space Flight Center (320 kg m⁻³; Kurtz et al., 2014).

For the 'evolving' method, we calculated a representative winter (Oct-Apr) densification rate using the average densification rate of snow at the North Pole given by W99. This was found to be approximately +6.45 kg m⁻³ per month. The October starting density was taken as the W99 October North Pole density - this choice served to minimise sea ice thickness bias at the start of the growth season and better enable comparison of growth rate. Snow density in the 'evolving' method can therefore be written as:

$$\rho_s = 6.45t + 275.3 \quad (11)$$

Where t represents the number of months since October.

The North Pole was chosen for two reasons: its density evolution can be trivially read from the published data in W99 and it suffers least from edge effects due to the quadratic fitting. To further justify this choice, the W99 snow density evolution of five Arctic regions were also examined and found to be similar to the North Pole rate, with the exception of the Laptev Sea which shows only a small (but positive) seasonal densification rate (Fig. S3). As in Sect. 2, we halved the W99 snow depths over FYI and only analysed the Central Arctic basin where W99 is considered most reliable. When the evolving density shown in Eq. (11) was included in our calculation of the radar wave propagation correction, we found sea ice thickness to grow on average by an extra 10.1 cm between October and April over MYI. This corresponds to an extra 1.7 cm per month when compared to a fixed $f(c_s)$ of 0.25Z. Density evolution caused FYI to grow an extra 6.4 cm over the same time period, corresponding to an extra 1.1 cm per month.

Given the poor state of knowledge concerning the current distribution of pan-Arctic snow densities and the difficulty in collecting in-situ data, we cannot conclude whether this increased growth should correspond to higher-than-previous thick-

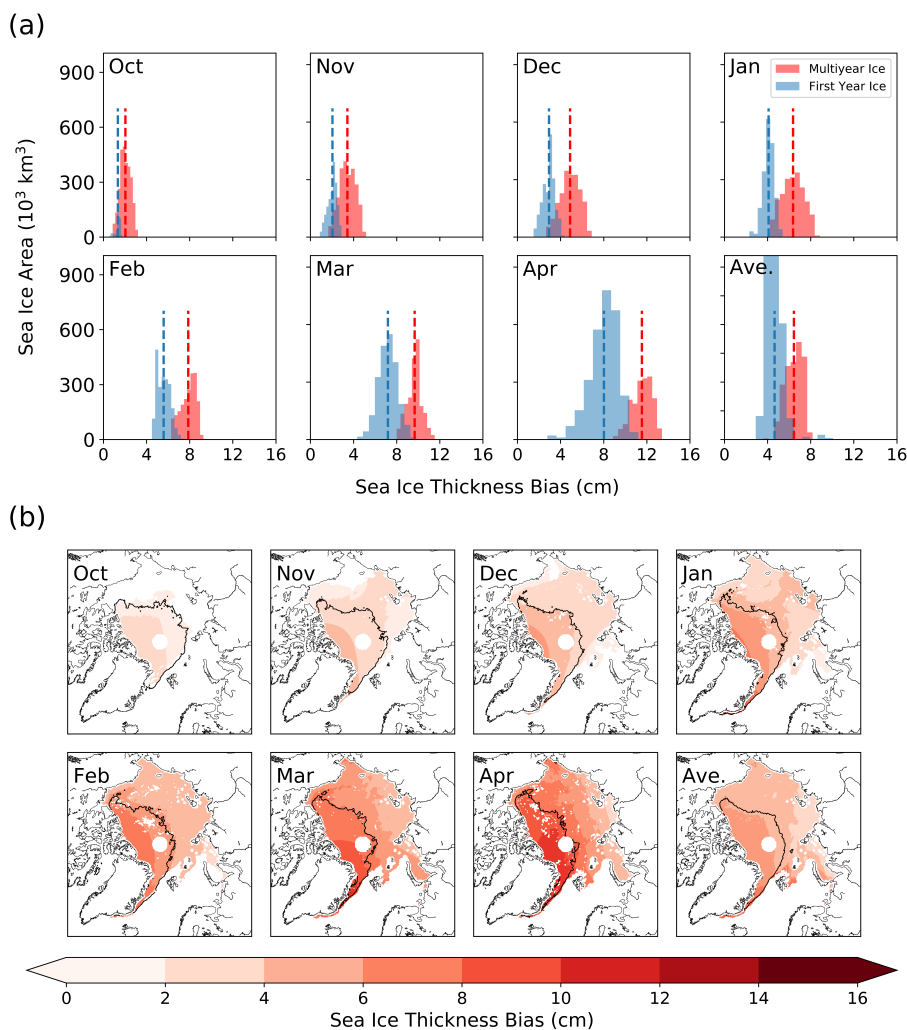


Figure 2. Monthly biases in sea ice thickness due to the effect of ignoring snow densification in calculating propagation correction (a) Spatially averaged histograms indicating the area of ice subjected to a given bias. Data separated into pixels that feature MYI for that month in more/less than 50% of years 2010-2018. Pixels that typically feature MYI experience greater bias in all months, largely due to halved W99 snow depths over FYI. (b) Bias maps illustrating sea ice thickness biases. Pixels are only displayed where sea ice type is known in all years 2010-2018, so bias is not displayed in some areas of ambiguous ice type. Black line indicates region where MYI is present in over 50% of years.

nesses at the end of winter or lower-than-previous thicknesses at the start of winter. Put another way, in this section we show a systematic bias in the growth rate rather than absolute thickness values.

Having illustrated the effect of snow densification on the radar wave propagation correction, we now justify its inclusion.



150 While the absolute values for regional mean densities have conceivably changed since the data was collected for W99, it remains almost certain that snow density still increases over winter for the majority of the Arctic basin as documented in W99. Furthermore, the rate of snow densification shown in W99 is likely now underestimated, with field observations indicating densification rates of $>20 \text{ kg m}^{-3}$ per month on FYI (Langlois et al., 2007) and FYI now occupying significantly more of the Arctic basin than in the 1954-91 period over which W99 was compiled (Stroeve and Notz, 2018). While significant uncertainty in the true densification rate exists, setting the rate to zero introduces a systematic bias in sea ice thickness calculations.

155 Finally, commonly used products (e.g. Tilling et al., 2018; Hendricks et al., 2016) have included snow density in the ‘snow loading correction’ (for change in the hydrostatic equilibrium of the floe due to the weight of snow cover), which features a very similar sensitivity to uncertainty in snow density (Fig. S4).

4 Discussion

4.1 Different Fixed Densities

160 To further explore this issue, we calculated the expected difference between sea ice thickness estimates from CPOM and AWI introduced by their usage of $\delta h = 0.25Z$ and $\delta h = 0.22Z$ respectively. Since the difference in δh is partially due to different choices of a representative snow density, resulting sea ice thickness differences cannot be seen as bias from a true value until Arctic snow densities are better constrained. This variation is superimposed on the bias introduced by fixed snow densities discussed above. We find that CPOM’s higher value for $f(c_s)$ produces a higher mean MYI thickness of 5cm in November, growing to 7cm by April. 16% of MYI exhibited a difference of > 8 cm. For FYI, the mean difference is 2.8 cm in November
165 and grows to 4.7cm by April (Fig. S5).

4.2 Comparison to Radar Freeboards

To investigate these biases further, we compare them by converting pan-Arctic CryoSat-2 radar freeboard retrievals from late 2010 to early 2018 from Landy et al. (2019, In Review) to estimates of sea ice freeboard using:

- 170
- Equation (5) versus Eq. (6) (with conventional, erroneous interpretation) using the depth and density fits from W99
 - A monthly evolving density versus the fixed density used in Hendricks et al. (2016), both with spatially constant density across the Arctic basin

We find that the bias induced by the conventional, erroneous interpretation of Eq. (6) remains relatively constant as a fraction of the sea ice freeboard at around 6% (despite increasing in an absolute sense) (Fig. 3a).

175 We find that the bias induced by the assumption of a non-evolving snow density (in calculation of the propagation offset) grows throughout the season relative to the sea ice freeboard and in an absolute sense. The bias grows from 2.3% to 6% of the ice freeboard (Fig. 3b), indicating that the growth rate is underestimated when a fixed density is assumed.

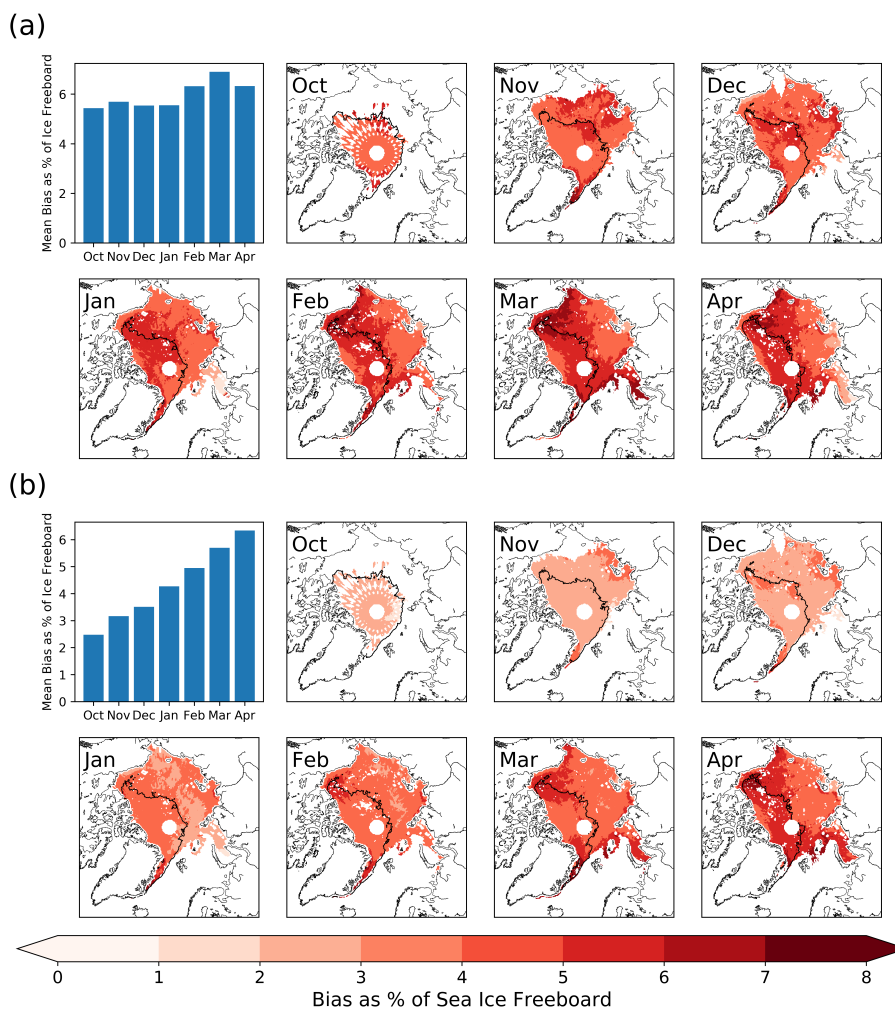


Figure 3. Percentage bias in sea ice freeboard. The bias induced by two effects was compared to the ice freeboards from Landy et al (2019, In Review). (a) Percentage bias introduced by the use of Eq. (5) vs Eq. (6) when combined with the W99 fits for depth and density. As a fraction of the growing ice freeboard, biases remain relatively constant, indicating they grow at the same rate. (b) Percentage bias introduced by an evolving snow density derived from the densification rate at the North Pole. This bias increases as a fraction of the ice freeboard from 2.3% to >6%, indicating that thermodynamic growth rates are underestimated.

4.3 Broader Implications

Sea ice thickness is closely tied to sea ice volume, a sensitive indicator of climate change but also a quantity of major interest for the modelling community. The thickness underestimates highlighted in Sect. 2 have some impact on total sea ice volume, although this is well within the currently large uncertainty bounds. Nonetheless, we argue that these uncertainty bounds have been systematically biased low through conventional use of Eq. (6) in some products.



In addition, the fact that these underestimates grow over winter means the seasonal growth rate is also underestimated through conventional use of Eq. (6). While the rate of winter sea ice growth is still uncertain and interannually variable, the use of a fixed, seasonally-constant value for the snow density will bias growth rates low.

Accurate characterisation of thermodynamic growth is important to a variety of systems. A higher growth-rate will impact the surface salinity balance as more freshwater than previously estimated is locked up in sea-ice during thermodynamic growth and then ejected to the mixed-layer when ice melts in summer. The rate of sea ice growth is an important variable in the characterization of the negative conductive feedback (thin ice thickens faster: Stroeve et al., 2018; Petty et al., 2018a). Finally, end of winter sea ice thickness moderates subsequent light transmittance through the ice, impacting under-ice ecosystems and related geochemical processes (Nicolaus et al., 2012).

Sea ice thickness products featuring the misinterpretations of Eq. (6) have fed several forecast and reanalysis models (e.g. Xia and Xie, 2018). Thickness products featuring a constant-density assumption are near-ubiquitous and have also fed forecast and reanalysis models (e.g. Yaremchuk et al., 2019; Blockley and Peterson, 2018). While these biases may be small compared to the effects of partial radar penetration into the snow cover as a function of snow pack variables (e.g. salinity, wetness, temperature), they are remediable and can be simply applied before further work is undertaken to correct radar range estimates for partial penetration of the wave into the snow cover.

4.4 Summary

We investigated two conventional methods for correcting radar altimetry based sea ice freeboard retrievals for slower radar wave propagation in snow. We found that a commonly used treatment (conventional use of Eq. (6)) for this correction leads to initial and seasonally-increasing underestimation of sea ice thickness from October through to April. While most commonly-used products then transform this bias (where present) by choosing a fixed snow density, we find underestimation of April sea ice thickness to exceed 15 cm over some multiyear ice when this treatment is applied in conjunction with the snow climatology from Warren et al. (1999).

We also investigated the impact of assuming a seasonally-fixed snow density on the radar wave propagation correction. While uncertainties in the absolute value of Arctic snow density preclude any conclusion about whether sea ice thickness is being under- or overestimated in this respect, the thermodynamic growth rate of multiyear ice is found to be underestimated by ~ 1.7 cm per month leading to a ~ 10.1 cm underestimate in growth over the October-April period.

While these biases in sea ice thickness (Sect. 2) and growth rate (Sections 2 & 3) are small compared to the total uncertainty, they are systematic and influence the uncertainty bounds. These biases also propagate into derived products and model projections, calibrations and reanalyses.

Code and data availability. https://github.com/robbiemallett/snow_density_assumptions



Author contributions. RDCM carried out the analysis and wrote the manuscript, with continued input from all authors. In addition to manuscript input, JCS and JCL contributed data to aid analysis and MCT contributed to the processing code.

215 *Competing interests.* The authors declare no competing interests.

Acknowledgements. This work was funded primarily by the London Natural Environmental Research Council Doctoral Training Partnership grant (NE/L002485/1). JCL acknowledges support from the European Space Agency Living Planet Fellowship ‘Arctic-SummIT’ under grant ESA/4000125582/18/I-NS and the Natural Environmental Research Council Project ‘Diatom-ARCTIC’ under Grant NE/R012849/1. MT acknowledges support from the European Space Agency in part by project ‘Polarice’ under grant ESA/AO/1-9132/17/NL/MP and in part by
220 the project ‘CryoSat + Antarctica’ under Grant ESA AO/1-9156/17/I-BG.



References

- Aaboe, S., Breivik, L.-A., Sørensen, A., Eastwood, S., and Lavergne, T.: Global sea ice edge and type product user's manual, OSI-403-c & EUMETSAT, 2016.
- Armitage, T. W. and Ridout, A. L.: Arctic sea ice freeboard from AltiKa and comparison with CryoSat-2 and Operation IceBridge, *Geophysical Research Letters*, 42, 6724–6731, 2015.
- Blockley, E. W. and Peterson, K. A.: Improving Met Office seasonal predictions of Arctic sea ice using assimilation of CryoSat-2 thickness, *The Cryosphere*, 12, 3419–3438, 2018.
- Chan, P., Halfar, J., Adey, W., Hetzinger, S., Zack, T., Moore, G., Wortmann, U., Williams, B., and Hou, A.: Multicentennial record of Labrador Sea primary productivity and sea-ice variability archived in coralline algal barium, *Nature communications*, 8, 15 543, 2017.
- Day, J., Hawkins, E., and Tietsche, S.: Will Arctic sea ice thickness initialization improve seasonal forecast skill?, *Geophysical Research Letters*, 41, 7566–7575, 2014.
- Graham, R. M., Cohen, L., Petty, A. A., Boisvert, L. N., Rinke, A., Hudson, S. R., Nicolaus, M., and Granskog, M. A.: Increasing frequency and duration of Arctic winter warming events, *Geophysical Research Letters*, 44, 6974–6983, 2017.
- Hallikainen, M., Ulaby, F., and Abdel-Razik, M.: Measurements of the dielectric properties of snow in the 4-18 GHz frequency range, in: 1982 12th European Microwave Conference, pp. 151–156, IEEE, 1982.
- Hendricks, S., Ricker, R., and Helm, V.: User Guide - AWI CryoSat-2 Sea Ice Thickness Data Product (v1.2), 2016.
- Kurtz, N. T., Galin, N., and Studinger, M.: An improved CryoSat-2 sea ice freeboard retrieval algorithm through the use of waveform fitting, *The Cryosphere*, 8, 1217–1237, 2014.
- Kwok, R.: Simulated effects of a snow layer on retrieval of CryoSat-2 sea ice freeboard, *Geophysical Research Letters*, 41, 5014–5020, 2014.
- Kwok, R.: Arctic sea ice thickness, volume, and multiyear ice coverage: losses and coupled variability (1958–2018), *Environmental Research Letters*, 13, 105 005, 2018.
- Kwok, R. and Cunningham, G.: Variability of Arctic sea ice thickness and volume from CryoSat-2, *Philosophical Transactions of the Royal Society A: Mathematical, Physical and Engineering Sciences*, 373, 20140 157, 2015.
- Kwok, R., Panzer, B., Leuschen, C., Pang, S., Markus, T., Holt, B., and Gogineni, S.: Airborne surveys of snow depth over Arctic sea ice, *Journal of Geophysical Research: Oceans*, 116, 2011.
- Landy, J. C., Ehn, J. K., Babb, D. G., Thériault, N., and Barber, D. G.: Sea ice thickness in the Eastern Canadian Arctic: Hudson Bay Complex & Baffin Bay, *Remote sensing of environment*, 200, 281–294, 2017.
- Langlois, A., Mundy, C., and Barber, D. G.: On the winter evolution of snow thermophysical properties over land-fast first-year sea ice, *Hydrological Processes: An International Journal*, 21, 705–716, 2007.
- Laxon, S., Peacock, N., and Smith, D.: High interannual variability of sea ice thickness in the Arctic region, *Nature*, 425, 947, 2003.
- Laxon, S. W., Giles, K. A., Ridout, A. L., Wingham, D. J., Willatt, R., Cullen, R., Kwok, R., Schweiger, A., Zhang, J., Haas, C., et al.: CryoSat-2 estimates of Arctic sea ice thickness and volume, *Geophysical Research Letters*, 40, 732–737, 2013.
- Nicolaus, M., Katlein, C., Maslanik, J., and Hendricks, S.: Changes in Arctic sea ice result in increasing light transmittance and absorption, *Geophysical Research Letters*, 39, 2012.
- Petty, A. A., Holland, M. M., Bailey, D. A., and Kurtz, N. T.: Warm Arctic, Increased Winter Sea Ice Growth?, *Geophysical Research Letters*, 45, 12–922, 2018a.



- Petty, A. A., Webster, M., Boisvert, L., and Markus, T.: The NASA Eulerian Snow on Sea Ice Model (NESOSIM) v1. 0: initial model development and analysis., *Geoscientific Model Development*, 11, 2018b.
- 260 Ricker, R., Hendricks, S., Perovich, D. K., Helm, V., and Gerdes, R.: Impact of snow accumulation on CryoSat-2 range retrievals over Arctic sea ice: An observational approach with buoy data, *Geophysical Research Letters*, 42, 4447–4455, 2015.
- Schweiger, A. J.: Unified Sea Ice Thickness Climate Data Record, Polar Science Center, Applied Physics Laboratory, University of Washington, http://psc.apl.uw.edu/sea_ice_cdr, accessed on 09/9/2019, 2017.
- Sévellec, F., Fedorov, A. V., and Liu, W.: Arctic sea-ice decline weakens the Atlantic meridional overturning circulation, *Nature Climate Change*, 7, 604, 2017.
- 265 Stroeve, J. and Notz, D.: Changing state of Arctic sea ice across all seasons, *Environmental Research Letters*, 13, 103 001, 2018.
- Stroeve, J. C., Schroder, D., Tsamados, M., and Feltham, D.: Warm winter, thin ice?, *The Cryosphere*, 12, 1791–1809, 2018.
- Tilling, R. L., Ridout, A., and Shepherd, A.: Estimating Arctic sea ice thickness and volume using CryoSat-2 radar altimeter data, *Advances in Space Research*, 62, 1203–1225, 2018.
- 270 Tiuri, M., Sihvola, A., Nyfors, E., and Hallikaiken, M.: The complex dielectric constant of snow at microwave frequencies, *IEEE Journal of oceanic Engineering*, 9, 377–382, 1984.
- Ulaby, F. T., Moore, R. K., and Fung, A. K.: *Microwave remote sensing: Active and passive. Volume 3-From theory to applications*, 1986.
- Warren, S. G., Rigor, I. G., Untersteiner, N., Radionov, V. F., Bryazgin, N. N., Aleksandrov, Y. I., and Colony, R.: Snow depth on Arctic sea ice, *Journal of Climate*, 12, 1814–1829, 1999.
- Wingham, D., Francis, C., Baker, S., Bouzinac, C., Brockley, D., Cullen, R., de Chateau-Thierry, P., Laxon, S., Mallow, U., Mavrocordatos, 275 C., et al.: CryoSat: A mission to determine the fluctuations in Earth’s land and marine ice fields, *Advances in Space Research*, 37, 841–871, 2006.
- Xia, W. and Xie, H.: Assessing three waveform retracers on sea ice freeboard retrieval from Cryosat-2 using Operation IceBridge Airborne altimetry datasets, *Remote Sensing of Environment*, 204, 456–471, 2018.
- Yaremchuk, M., Townsend, T., Panteleev, G., Hebert, D., and Allard, R.: Advancing Short-Term Forecasts of Ice Conditions in the Beaufort 280 Sea, *Journal of Geophysical Research: Oceans*, 2019.